Structural investigation of tungsten oxide nanowires by X-ray diffraction and transmission electron microscopy

Shibin Sun, Suyuan Sun, and Zhenjiang Li[a)]
College of Electromechanical Engineering, Qingdao University of Science and Technology, Qingdao 266061, Shandong, People's Republic of China

(Received 14 June 2010; accepted 18 June 2010)

X-ray diffraction, selected area electron diffraction, and high-resolution transmission electron microscope techniques were used to investigate the crystalline structures of one-dimensional tungsten oxide nanowires prepared by the hydrothermal method. The as-synthesized products were found to exhibit increasing crystallinity with increasing reaction time, and tungsten oxide nanowires have crystalline defects, including stacking faults, dislocations, and vacancies. The results on the crystal defects help us to obtain a better understanding of the temperature-dependent morphological evolution of the ultrathin nanowires synthesized under different thermal processes. © *2010 International Centre for Diffraction Data.* [DOI: 10.1154/1.3478559]

Key words: tungsten oxide, nanowire, XRD, SAED, HRTEM

I. INTRODUCTION

In the past few years, one-dimensional (1D) nanostructured materials have attracted tremendous research interest owing to their unique physical, chemical, and optical properties (Shankar *et al.*, 2007; Xia *et al.*, 2003; Baeck *et al.*, 2003). Among all nanomaterials, tungsten oxides are of much importance because of their outstanding electrochromic, gaschromic, thermochromic, and optochromic properties, as well as their potential applications in electrochromic display, semiconductor gas sensors, and photocatalysts (Sanrato *et al.*, 2001; Pol *et al.*, 2005; Wang *et al.*, 2009). Particularly, 1D tungsten oxide can be used as a precursor for the preparation of tungsten disulfide nanotubes. As one important specie of the inorganic fullerenelike materials, tungsten disulfide nanotubes have many potential applications in electron device, catalyst, superior solid lubricant, and high performance composite (Tenne *et al.*, 1992; Rothschild *et al.*, 2000). In a previous paper, we successfully prepared substoichiometric tungsten oxide nanowires by using a solution-based soft-chemistry method, and their features under thermal processing were systematically investigated (Sun *et al.*, 2008). In this paper, we present an in-depth morphological and structural analysis on tungsten oxide nanowires using X-ray diffraction (XRD), selected area electron diffraction (SAED), and high-resolution transmission electron microscope (HRTEM) techniques.

II. EXPERIMENTAL

Bundled tungsten oxide nanowires were successfully synthesized by using a hydrothermal method with hexachloride and cyclohexanol as raw materials (Sun *et al.*, 2008). First, 80 mg of WCl_6 was dissolved in 2 ml of ethanol in a beaker to obtain a solution. 60 ml of cyclohexanol was then added to the solution, which was subsequently transferred to and sealed in a PTFE-line 120 ml autoclave. The reaction times in our experiments were from 6 to 24 h. After natural cooling to room temperature, the precipitate was removed from the autoclave and then centrifuged and washed with de-ionized water and acetone several times. The resulting products were then characterized by an X-ray diffractometer (Siemens D500, Cu $K\alpha$ radiation), a transmission electron microscope (TEM) (JEOL 2000FX, 200 KV), and a HRTEM (JEOL 4000FX, 400 KV).

III. RESULTS AND DISCUSSION

TEM results show that the resulting products, synthesized at a WCl_6 concentration of 0.003*M* and with a reaction time of 6 h, exhibit bundled features with lengths up to a few microns and diameters of about 5 to 20 nm [see Figure 1(a)]. Detailed information on the nanowires characterization was previously reported by Sun *et al.* (2008). Large different morphologies but only slightly different crystalline structures, depending on the concentration of WCl_6 in cyclohexanol, have also been reported by Sun *et al.* (2009).

Both the morphologies and the crystalline structures of the hydrothermal products obtained in this study vary with different reaction times. As shown in the bottom XRD pattern of Figure 2, for a short reaction time of 5 h, only a couple of weak diffraction peaks at 23.5° and 48.0° 2θ can be assigned to the monoclinic $W_{18}O_{49}$ (010) and (020) reflections, respectively (Lamire *et al.*, 1987). The broad and

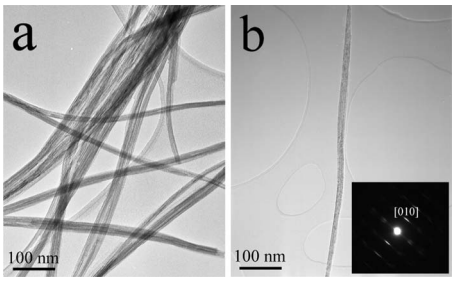

Figure 1. TEM images of the product synthesized with a reaction time of 6 h: (a) bundled $W_{18}O_{49}$ nanowires and (b) single $W_{18}O_{49}$ nanowire. The inset in Figure 1(b) is the SAED pattern.

[a)]Author to whom correspondence should be addressed. Electronic mail: zjli26@126.com

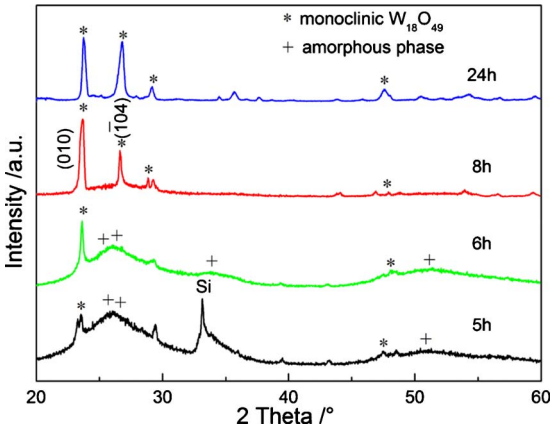

Figure 2. (Color online) XRD patterns of the as-synthesized products with different reaction times.

diffuse peak with a peak intensity appeared at around $27°2\theta$ can be attributed to the presence of an amorphous phase. The XRD results indicate that the resulting product has very poor degree of crystallinity. Increasing the reaction time to 6 h, the $W_{18}O_{49}$ (010) peak becomes much sharper and stronger than that of the product obtained with a reaction time of 5 h, indicating that the $W_{18}O_{49}$ ⟨010⟩ direction is the dominant growth direction for the ultrathin nanowires. Meanwhile, the intensities of the amorphous phase become significantly weaker suggesting that a part of the amorphous phase had transformed into crystalline $W_{18}O_{49}$ (see the XRD pattern of the 6 h product in Figure 2). Increasing the reaction time further to 8 h, the XRD pattern is dominated by sharp and intensive diffraction peaks of monoclinic $W_{18}O_{49}$, while the broad amorphous peak at $27°2\theta$ becomes almost invisible (see the XRD pattern for the 8 h product in Figure 2). Increasing the reaction time even further to 24 h, the $W_{18}O_{49}$ diffraction peaks are very strong, and no amorphous peak can be detected in the XRD pattern shown at the top of Figure 2. It should also be noted that the peak intensity of the $W_{18}O_{49}$ ($\bar{1}04$) reflection is also very strong similar to that of the strongest (010) peak, suggesting that the one-dimensional nanostructured feature in the hydrothermal product may likely disappear when the reaction time increases to 24 h. In fact, a mixture of irregular particles and thick rods was observed in the product with the reaction time of 24 h (not shown here).

After thorough dispersion by a sonication treatment, the bundled nanowires [shown in Figure 1(a)] can be dispersed to single flexible nanowires, and one of the nanowires is shown in Figure 1(b). The SAED pattern [bottom right inset; Figure 1(b)] of the nanowire exhibits a row of well-defined spots running parallel to the nanowire growth axis with a basic lattice spacing of ~0.38 nm and other rows of weak streak spots running nearly normal to the growth axis. The presence of the streak spots suggests the existence of crystal defects, such as dislocations, stacking faults, and/or oxygen vacancies. The HRTEM image shown in Figure 3(a) indicates that the lattice fringe separation is ~0.38 nm for the (010) lattice plane of monoclinic $W_{18}O_{49}$, in agreement with the SAED and XRD results. A very thin amorphous layer can also be seen [see the black arrow in Figure 3(a)], confirming the XRD results. Moreover, HRTEM can give detailed information on possible defects presented in a nanowire. For example, by a careful examination of the squared areas in Figure 3(a), edge dislocations or stacking faults can be clearly observed [see the white arrows shown in Figures 3(b) and 3(c)]. It is also worth pointing out that discontinuities of lattice fringe are presented in a larger nanowire. The presence of the observed discontinuities may be caused by a combination of the oxygen vacancies in substoichiometric $W_{18}O_{49}$ and an incomplete crystallization during the hydrothermal process. The crystal defects shown in the HRTEM images also correlated with the streaking spots in the SAED patterns [see Figure 1(b)].

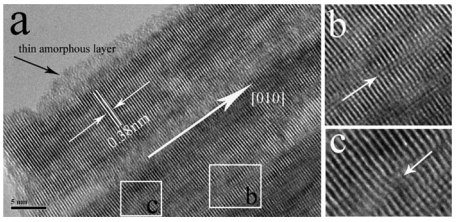

Figure 3. HRTEM image of a $W_{18}O_{49}$ nanowire shown in Figure 1(b). Figures 3(b) and 3(c) are the high magnification images of the corresponding sections in Figure 3(a).

The bundled tungsten oxide nanowires gradually undergo a series of morphological evolution with increased temperature, as reported in earlier works by Sun *et al.* (2008, 2009). Based on HRTEM results obtained in this study, we propose a possible defect-induced mechanism. During thermal processing, crystal defects are highly activated after absorbing external energy and favor a morphological transformation of the nanowires. Hence, the defect-located areas will possibly be the preferential evolution source, especially the locations where individual nanowires are intersected within the bundles. With increasing temperature, the neighboring defective sites between single nanowires will then be combined, fractured, or broken, finally resulting in the apparent morphological evolution.

IV. CONCLUSION

In summary, the crystalline structures of the hydrothermal products with different reaction times were studied, and the structural analysis of the tungsten oxide nanowires using X-ray diffraction and transmission electron microscopy was also performed. The as-synthesized products exhibit increasing degree of crystallinity with increasing reaction time. It was found that the single dispersed nanowire has crystal defects, including stacking faults, edge dislocations, and/or oxygen vacancies. The results obtained in this study provide a better understanding of the temperature-dependent morphological evolution of the ultrathin nanowires under thermal processing, which can be beneficial to define the working environment for their potential applications.

ACKNOWLEDGMENTS

This work was supported by the National Natural Science Foundation of China under Grant Nos. 50972063 and 50572041, the Natural Science Foundation of Shandong

https://doi.org/10.1154/1.3478559 Published online by Cambridge University Press

Province under Grant No. Y 2007F 64, the Science and Research Development Plan of Education Department in Shandong Province under Grant No. J 06A 02, the Tackling Key Program of Science and Technology in Shandong Province under Grant No. 2006GG2203014, and the Application Foundation Research Program of Qingdao under Grant No. 09-1-3-27-jch.

Baeck, S. H., Choi, K. S., Jaramillo, T. F., Stucky, G. D., and McFarland, E. W. (**2003**). "Enhancement of photocatalytic and electrochromic properties of electrochemically fabricated mesoporous WO_3 thin films," Adv. Mater. **15**, 1269–1273.

Lamire, M., Labbe, P., Goreaud, M., and Raveau, B. (**1987**). "Refinement and new structure analysis of W18O49," Rev. Chim. Miner. **24**, 369–381.

Pol, S. V., Pol, V. G., Kessler, V. G., Seisenbaeva, G. A., Solovyov, L. A., and Gedanken, A. (**2005**). "Synthesis of WO_3 nanorods by reacting $WO(OMe)_4$ under autogenic pressure at elevated temperature followed by annealing," Inorg. Chem. **44**, 9938–9945.

Rothschild, A., Sloan, J., and Tenne, R. (**2000**). "Growth of WS_2 nanotubes phases," J. Am. Chem. Soc. **122**, 5169–5179.

Sanrato, C., Odziemkowski, M., Ulmann, M., and Augustynski, J. (**2001**). "Crystallographically oriented mesoporous WO_3 films: Synthesis, characterization, and applications," J. Am. Chem. Soc. **123**, 10639–10649.

Shankar, K., Mor, G. K., Fitzzgerald, A., and Grimes, C. A. (**2007**). "Cation effect on the electrochemical formation of very high aspect ratio TiO_2 nanotube arrays in formamide-water mixtures," J. Phys. Chem. C **111**, 21–26.

Sun, S. B., Zhao, Y. M., Xia, Y. D., Zou, Z. D., Min, G. H., and Zhu, Y. Q. (**2008**). "Bundled tungsten oxide nanowires under thermal processing," Nanotechnology **19**, 305709 (7pp).

Sun, S. B., Zou, Z. D., and Min, G. H. (**2009**). "Synthesis of bundled tungsten oxide nanowires with controllable morphology," Mater. Charact. **60**, 437–440.

Tenne, R., Margulis, L., Genut, M., and Hodes, G. (**1992**). "Polyhedral and cylindrical structures of tungsten disulphide," Nature (London) **360**, 444–446.

Wang, J. M., Lee, P. S., and Ma, J. (**2009**). "Synthesis, growth mechanism and room-temperature blue luminescence emission of uniform WO_3 nanosheets with W as starting material," J. Cryst. Growth **311**, 316–319.

Xia, Y. N., Yang, P. D., Sun, Y. G., Wu, Y. Y., Mayers, B., Gates, B., Yin, Y. D., Kim, F., and Yan, H. Q. (**2003**). "One-dimensional nanostructures: Synthesis, characterization, and applications," Adv. Mater. **15**, 353–389.